NANO LETTERS

pubs.acs.org/NanoLett

20 μs Photocurrent Response from Lithographically Patterned Nanocrystalline Cadmium Selenide Nanowires

Sheng-Chin Kung, Wytze E. van der Veer, Fan Yang, Keith C. Donavan, and Reginald M. Penner*

Department of Chemistry, University of California, Irvine, California 92697-2025

ABSTRACT Lithographically patterned nanowire electrodeposition (LPNE) provides a method for patterning nanowires composed of nanocrystalline cadmium selenide (*nc*-CdSe) over wafer-scale areas. We assess the properties of (*nc*-CdSe) nanowires for detecting light as photoconductors. Structural characterization of these nanowires by X-ray diffraction and transmission electron microscopy reveals they are composed of stoichiometric, single phase, cubic CdSe with a mean grain diameter of 10 nm. For *nc*-CdSe nanowires with lengths of many millimeters, the width and height dimensions could be varied over the range from 60 to 350 nm (w) and 20 to 80 nm (h). Optical absorption and photoluminescence spectra for *nc*-CdSe nanowires were both dominated by band-edge transitions. The photoconductivity properties of *nc*-CdSe nanowire arrays containing ~350 nanowires were evaluated by electrically isolating 5 μm nanowire lengths using evaporated gold electrodes. Photocurrents, i_{photo}, of 10−100 × (i_{dark}) were observed with a spectral response characterized by an onset at 1.75 eV. i_{photo} response and recovery times were virtually identical and in the range from 20 to 40 μs for 60 × 200 nm nanowires.

KEYWORDS Cadmium selenide, photoconductor, nanowire, electrodeposition, LPNE

In pursuit of photodetectors that are fast, sensitive, and small, the photoconductivity of semiconductor nanowires has been intensively studied but nanowire-based photoconductors capable of high bandwidth (>10 kHz) response to light intensity variations have proven to be difficult to achieve. Yang and co-workers reported the first photoconductivity measurements of single crystalline zinc oxide (ZnO)[1] and tin oxide (SnO_2)[2] nanowires in 2002. These nanowires produced large photocurrents but the diminished resistance of the illuminated nanowire was slow to recover in the dark, requiring more than 10 s to do so. Since 2002, the photoconductivity behavior of a wide variety of single crystalline nanowires has been examined, including ZnO,[1,3−11] SnO_2,[2,12,13] gallium nitride (GaN),[14,15] cadmium sulfide (CdS),[16−20] and cadmium selenide (CdSe),[21−23] and slow photocurrent recovery has been seen, to various extents, in all of these systems.[1−15,18] A mechanism proposed to account for slow photocurrent recovery in GaN nanowires[24] is the presence of a carrier depletion layer at the wire surface caused by fixed surface charge. The separation of photoexcited electron−hole pairs across the e-field coincident with this layer prevents recombination and retards the recovery rate in the dark.[24] For ZnO nanowires, this same e-field favors the migration of holes to the wire surface where they react: $O_2^-(ads) + h^+ \rightarrow O_2(g)$, and the kinetics of this chemical reaction further retards the rate at which the nanowire equilibrates after exposure to light.[1,4,6,25] The fastest photoconductive ZnO nanowires are those recently described by Wang and co-workers[4] where Schottky contacts to the nanowire were employed. Those nanowires showed a recovery time constant as short as 20 ms.[4]

Somewhat faster photoconductivity performance has been obtained for cadmium chalcogenide nanostructures (Table 1) in a few cases: Jie et al.[16] measured response and recovery times of 750−800 μs for CdS nanoribbons that were micrometers in width but just 2−40 nm in height. Liu et al.[17] also studied CdS nanoribbons with widths of micrometers and heights of 65 nm, observing response and recovery times of 500−1000 μs. CdSe nanoribbons producing response and recovery times in the 1−10 ms range, the most rapid observed to date for this material, have been reported by Jiang et al.[22] (Table 1) Kuno, Jena, and co-workers have studied the photoconductivity of randomly oriented ensembles of CdSe single crystalline nanowires in some detail,[26−28] focusing especially on the photocurrent sensitivity to optical polarization of the incident light. Remarkably, despite their random orientation, these nanowire ensembles produced a significant polarization anisotropy at polarization modulation frequencies up to 100 Hz in these studies.[28]

Polycrystalline CdSe films (Table 1) can produce 200−1000 μs response and recovery times[29,30] significantly faster, we believe, than any single crystalline nanowires studied to date. Inspired by these results, we have sought to synthesize and characterize the photoconductivity of polycrystalline II−VI nanowires. Mallouk and co-workers[23] found that single, polycrystalline, 350 nm diameter CdSe nanowires

* To whom correspondence should be addressed.
Received for review: 02/9/2010
Published on Web: 03/24/2010

DOI: 10.1021/nl100483v | *Nano Lett.* **2010,** *10,* 1481–1485

TABLE 1. Summary of Photoconductivity Performance Metrics for Cadmium Chalcogenide Nanostructures and Thin Films

material[a]	response, recovery[b]	photosensitivity[c]	dimensions[d]	ref
CdSe film	1.0 ms, 1.5 ms	$10-10^8$	40 μm (gap) × 2.2 mm (w) × 700 nm (h)	45
CdSe film	1.6 ms, 1.6 ms	11	0.5 cm (gap) × 2.0 cm (w) × 750 nm (h)	46
CdSe film	1.0 ms, 0.2 ms	10^6	35 μm (gap) × 10 μm (w) × 300 nm (h)	29
CdSe film	1.3 ms, 0.2 ms	n.a.	1 cm^2 (A) × 300 nm (h)	30
CdSe film	200 ms, 200 ms	10^3-10^7	5 mm (gap) × 5 mm (w) × 170 nm (h)	47
CdSe rod	1 s, 200 μs	15	350 nm (diameter)	23
CdS wires	~15 ms, ~15 ms	39	20 μm (gap) × 200 nm (dia.) array	20
CdS belt	1 s, 3 s	1.5×10^3	200 nm (w)	18
CdS ribbon	200 ms, 500 ms	2	25 μm (gap) × 640 nm (w) × 50 nm (h)	19
CdS ribbon	746 μs, 794 μs	9.2×10^3	18 μm (gap) × 10−60 μm (w) × 2−40 nm(h)	16
CdS ribbon	551 μs, 1.09 ms	3.3×10^6	50 nm (gap) × 5−10 μm (w) × 65 nm (h)	17
CdSe ribbon	1.7 ms, 6.7 ms	n.a	5 μm (gap) × 5 μm (w) × 60 nm (h)	22
CdSe wire	700 ms, 700 ms	40	3 μm (gap) × 60 nm (dia.)	21
CdTe rods	>1 s, >3 s	10	2 μm (gap) × 300 nm (dia.) vertical array	48
CdSe wires	20 μs, 30 μs	10−100	5 μm (gap) × 200 nm (w) × 60 nm (h) array	this work

[a] All photoconductivity data pertain to measurements carried out at room temperature in air. [b] Response and recovery times as defined by the authors. [c] Photosensitivity = $(\sigma_{light} - \sigma_{dark})/\sigma_{dark}$, where σ is the electrical conductivity. [d] (gap) indicates the electrically isolated wire or rod length, if specified.

produced a photocurrent characterized by 200 μs recovery. Earlier we[20] reported a study of nanocrystalline CdS nanowires, prepared by electrochemical step edge decoration, in which photocurrent response/recovery times in the 20 ms range were obtained. Here we use the lithographically patterned nanowire electrodeposition (LPNE) method[31−33] to prepare nanocrystalline CdSe (*nc*-CdSe) nanowires that produce photocurrent characterized by response and recovery times in the 20−40 μs range.

The LPNE process (Figure 1a,b) involves the fabrication by photolithography of a template consisting of a three-sided horizontal trench in which is embedded a vertical nickel nanoband electrode (Figure 1a,b(iii)).[31−33] In this study, a LPNE template was immersed in an aqueous plating solution containing the precursors Cd^{2+} (0.30 M $CdSO_4$) and SeO_3^{2-} (0.70 mM SeO_2) in aqueous 0.25 M H_2SO_4, pH = 1−2.[23,34−36] From this asymmetric plating solution, stoichiometric, single phase *nc*-CdSe nanowires were produced within the LPNE template using the scanning electrodeposition stripping method.[34−39] Briefly, cadmium-rich CdSe was first electrodeposited on the nickel electrode during a negative-going voltammetric scan to −0.8 V vs SCE (saturated calomel electrode, Figure 1c, bottom), and excess elemental cadmium was then stripped from the nascent nanowire on an ensuing postive-going voltammetric scan. The positive scan limit (−0.4 V vs SCE) is sufficiently negative to ensure that the electrodeposited CdSe does not oxidize. We prepared linear arrays of *nc*-CdSe nanowires at 5 μm pitch in this study (Figure 1d). The height of these nanowires, perpendicular to the glass substrate, is determined by the thickness of the nickel layer deposited in the first step of the LPNE process (Figure 1a,b(i)). A 60 nm thickness was used for all the nanowires investigated in this paper. The nanowire width is determined by the number of synthesis scans (Figure 1e,f). We studied the properties of nanowires with widths of 50 nm (1 scan), 100 nm (5 scans), and 200 nm (~20 scans). In all cases, these nanowires were subjected to thermal annealing (300 °C for 4 h in N_2) prior to structural or optical characterization. *nc*-CdSe nanowires adhered strongly to the glass surface even after annealing. The delamination of these nanowires from the glass was not observed in this study. The long-term stability of nanowire arrays was not investigated, but we observed no degradation in the photoresponse of nanowire arrays over periods of up to 1 month.

The nanocrystalline structure of these nanowires is immediately apparent from the transmission electron microscope (TEM) image of a single CdSe nanowire (Figure 2a−c). High magnification images (e.g., Figure 2c) reveal lattice fringes spaced by 0.350 nm corresponding to atomic planes along the [111] lattice direction of cubic CdSe. Both selected area electron diffraction (Figure 2d) and powder X-ray diffraction (Figure 2e) show multiple reflections that can also be assigned to cubic CdSe (JCPDS 88-2346). The grain diameter estimated from TEM analysis is ~10 nm while Scherrer analysis of the X-ray line width[40] provides a value of 9.2 nm (for the (111) reflection).

Absorbance and photoluminescence spectra for arrays of 60 nm × 200 nm *nc*-CdSe nanowires on glass (Figure 3a) both show optical transitions in the range from 1.74 to 1.76 eV, qualitatively as expected for bulk CdSe (E_g = 1.75 eV). The photoconductivity of these nanowires was investigated by electrically isolating 5 μm sections of approximately 350 nanowires deposited on glass by LPNE in a linear array at 5 μm pitch (Figure 3b). Current versus voltage plots for such arrays were Ohmic and chopped green illumination (532 nm at 91 mW/cm^2) produced photocurrents ranging from 10 to 100 × (i_{dark}) (e.g., Figure 3c). The spectral response of this photocurrent (Figure 3d) shows, with increasing photon energy, a sharp onset at 1.70 eV, a rapid increase to a peak at 2.20−2.30 eV, and a decline at higher photon energies, all qualitatively as previously observed for photoconductive films.[41]

The gain-bandwidth specification of the fast current amplifier used in these studies (Keithley 428-PROG) limited

DOI: 10.1021/nl100483v | *Nano Lett.* **2010,** *10,* 1481−1485

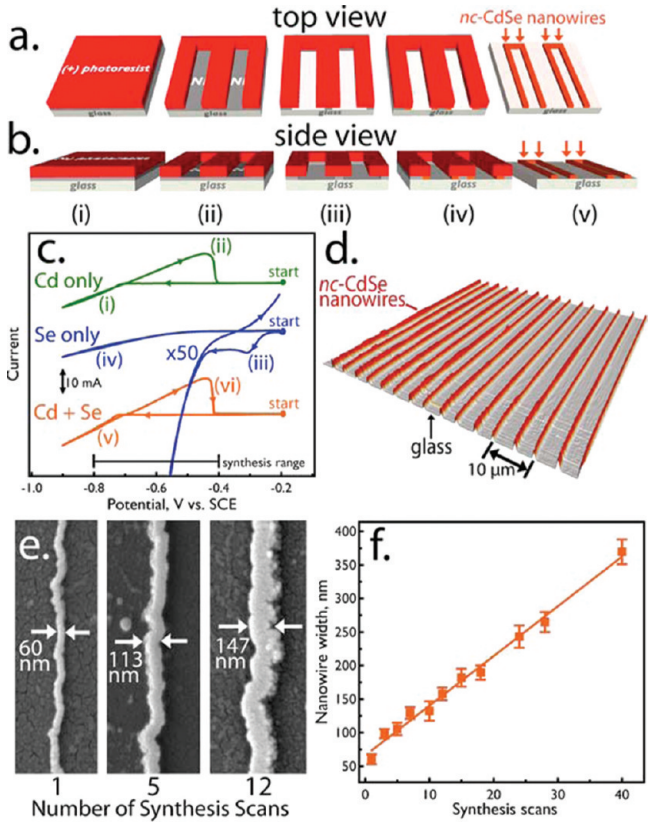

FIGURE 1. Synthesis of *nc*-CdSe nanowires. (a, b) Schematic diagram showing the five step process flow for the synthesis by LPNE of *nc*-CdSe nanowires: (i) a nickel layer and a (+)-photoresist (PR) layer are both deposited on a glass surface, (ii) the PR layer is patterned with a contact mask, (iii) nickel is etched from the patterned surface using nitric acid, (iv) *nc*-CdSe is electrodeposited from an aqueous solution containing both SeO_3^{2-} and Cd^{2+}. CdSe is deposited at the nickel electrodes—within the horizontal trench delineated on three sides by the PR, the glass surface, and the nickel electrodes. (v) PR and nickel are selectively removed to expose the *nc*-CdSe nanowires. (c) Cyclic voltammetry (50 mV/s) of plating solutions containing only Cd^{2+} (0.30 M, green), SeO_3^{2-} (0.70 mM, blue) and both precursors (orange). The electrolyte in all cases is 0.25 M H_2SO_4. The scan range used for the synthesis of *nc*-CdSe is indicated at bottom. Peak assignments for these voltammograms are as follows:

(peak i) $Cd^{2+} + 2e^- \rightarrow Cd(s)$,
$2H^+ + 2e^- \rightarrow H_2$;
(peak ii) $Cd(s) \rightarrow Cd^{2+} + 2e^-$;
(peak iii) $H_2SeO_3 + 4H^+ + 4e^- \rightarrow Se(s) + 3H_2O$;
(peak iv) $Se(s) + 2H^+ + 2e^- \rightarrow H_2Se$,
$H_2SeO_3 + 6H^+ + 6e^- \rightarrow H_2Se + 3H_2O$;
(peak v) $Cd^{2+} + Se(s) + 2e^- \rightarrow CdSe(s)$,
$Cd^{2+} + H_2SeO_3 + 4H^+ + 6e^- \rightarrow CdSe(s) + 3H_2O$,
$2H^+ + 2e^- \rightarrow H_2$;
(peak vi) $Cd(s) \rightarrow Cd^{2+} + 2e^-$.

(d) Atomic force micrograph of a 80 × 80 μm area of an array of *nc*-CdSe nanowires. (e) Scanning electron microscopy images of *nc*-CdSe nanowires prepared using 1, 5, and 12 synthesis scans. (f) Plot of mean nanowire width versus the number of synthesis scans.

single nanowire photoconductivity measurements to illumination modulation frequencies of 20−50 Hz for 60 nm × 200 nm *nc*-CdSe nanowires. By using 350 nanowires in parallel, the dark resistance, R, was reduced from the single nanowire value of ~4×10^{12} Ω to R/350 or 1×10^{10}Ω while

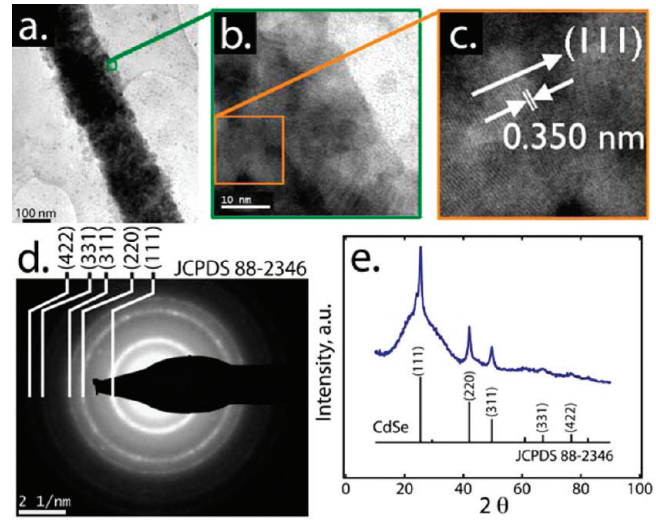

FIGURE 2. Structural characterization of *nc*-CdSe nanowires: a, b, c) transmission electron micrographs at progressively higher magnification showing the nanocrystalline grain structure, and ≈10 nm grain diameter, of individual *nc*-CdSe nanowires prepared by LPNE; (d) selected area electron diffraction pattern with indexing to cubic CdSe (JCPDS 88-2346); (e) grazing incidence X-ray powder diffraction pattern acquired for an array of *nc*-CdSe nanowires (60 nm (h) × 200 nm (w)) deposited at 5.0 μm pitch on glass. The broad diffraction peak seen at $2\theta = 25°$ derives from the glass surface. We index the four strongest reflections to cubic CdSe (JCPDS 88-2346) as indicated.

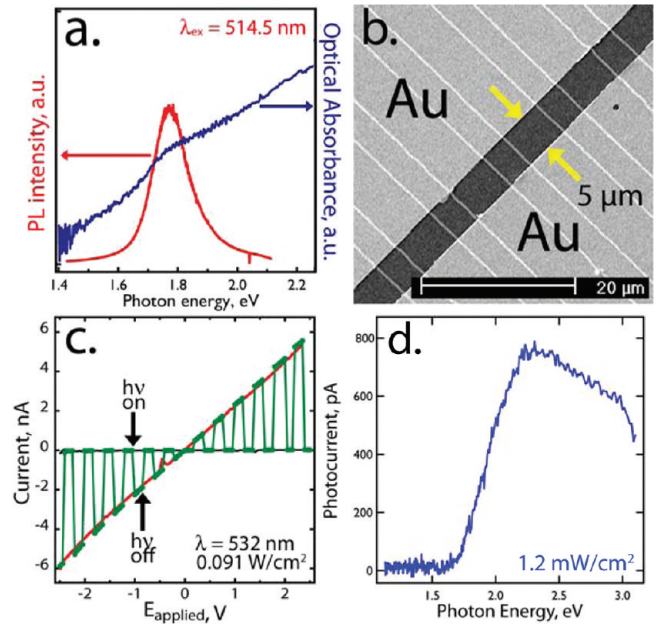

FIGURE 3. Characterization of the optical and photoconductivity properties of *nc*-CdSe nanowires: (a) an absorption spectrum (blue) for *nc*-CdSe patterned at 5 μm pitch on glass and a photoluminescence spectrum (red) for this same sample acquired with excitation at 514.5 nm; (b) scanning electron microscopy images showing the 5 μm gap employed for the photoconductivity measurements of *nc*-CdSe nanowire arrays studied in this paper, each array contained approximately 350 individual nanowires; (c) dark current (black) and photocurrent (red) versus applied bias for an array of 350 *nc*-CdSe nanowires. Also shown (green) is a current−voltage plot where the illumination (532 nm at 91 mW/cm^2) was periodically interrupted to switch between the dark (black) and illuminated (red) curves; (d) spectral response of the photocurrent for an array of 350 *nc*-CdSe nanowires biased as 1 V acquired using chopped illumination (350 Hz) with a mean power of 1.2 mW/cm^2.

DOI: 10.1021/nl100483v | *Nano Lett.* **2010,** *10,* 1481--1485

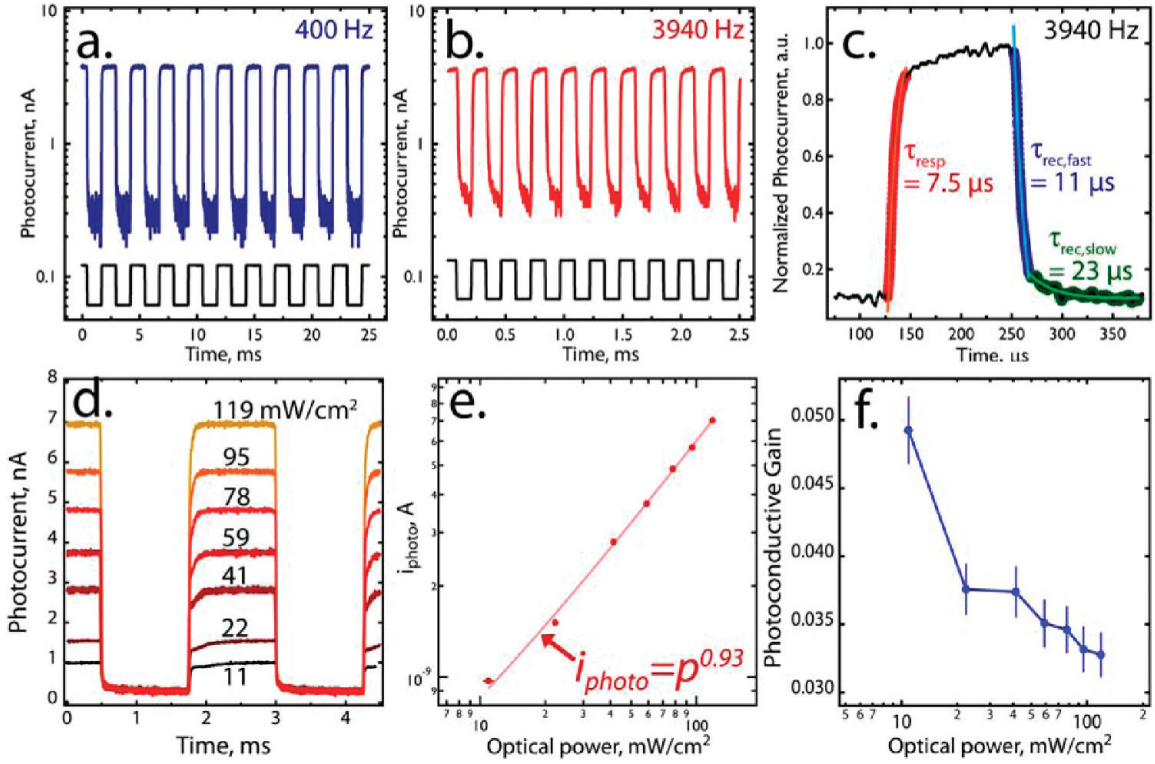

FIGURE 4. Photocurrent response and recovery for arrays of 350 *nc*-CdSe nanowires: (a, b) modulation of the photocurrent as a function of time in response to chopped illumination (532 nm, 59 mW/cm^2) at frequencies of (a) 400 Hz and (b) 3940 Hz, nanowires were biased at 2 V, the black trace (shown at bottom in each frame) is the current response to the chopped illumination produced by a silicon photodiode; (c) normalized photocurrent versus time showing three exponential fits and the associated time constants for the response (τ_{resp}) and recovery ($\tau_{rec,fast}$ and $\tau_{rec,slow}$) edges; (d) photocurrent, measured at 400 Hz, as a function of optical power as indicated; (e) photocurrent versus optical power, from the data shown in (d), also plotted is the best fit to the equation $i_{photo} = P_{optical}{}^x$ that is achieved for $x = 0.93$; (f) the estimated photoconductive gain, $G = (I_{photo}/P_{optical})(h\nu/q)$ as a function of optical power. In this calculation, it is assumed that 80% of the incident photons are absorbed and that 90% of the 350 nanowires present in each device are electrically continuous. The error bars represent the estimated error in this calculation based on these assumptions coupled with the noise present in the measurement.

simultaneously increasing the bandwidth for measurement of the photocurrent response by the same factor of 350. This parallelization of the measurement was required to enable the measurement of the response and recovery times for 60 nm × 200 nm *nc*-CdSe nanowires using frequencies of up to 3940 Hz. The photocurrent response of the 350 wire array to intensity modulation at 400 and 3940 Hz, for example, are shown in panels a and b of Figure 4, respectively. The photocurrent produced by the array follows the chopped illumination at both frequencies, albeit with ~20% rolloff of the gain, at the higher frequency. The response time, defined as the time necessary for the photocurrent to increase from (0.1) i_{peak} to (0.9) i_{peak}, is 20 μs in this case and the recovery time, defined analogously, is 30 μs (Figure 4c). In other experiments, response and recovery times were indistinguishable and in the range from 20 to 40 μs. These values are significantly shorter than the response and recovery times observed for all other nanowire systems to date, to our knowledge, and this response is also faster than previous measurements for polycrystalline CdSe films (Table 1). Smaller nanowires (60 nm × 50 nm and 60 nm × 100 nm) showed a somewhat slower response/recovery of ~100 μs limited, however, by the bandwidth of the measuring circuit because of their higher resistance. The 3 dB bandwidth is inversely related to the 10/90 rise time, t_{rise}, according to the relation: $f_{3dB} = 0.35/t_{rise}$.[16] Thus, the 3 dB bandwidth of 60 nm × 200 nm *nc*-CdSe nanowires arrays is 9−18 kHz.

The leading and trailing edges of a single modulation cycle measured at 3940 Hz were fit to the equations $I = I_0(1 - e^{t/\tau_{resp}})$ and $I = I_0[Ae^{t/\tau_{rec,fast}} + Be^{t/\tau_{rec,slow}}]$ to determine the time constants for response, τ_{resp}, and recovery, ($\tau_{rec,fast}$ and $\tau_{rec,slow}$), respectively (Figure 4c). A biexponential was used to characterize photocurrent recovery because two temporally distinct processes were detected in the photocurrent decay, as previously observed for CdS nanoribbons.[16] This analysis yielded values of $\tau_{resp} = 7-8$ μs, $\tau_{rec,fast} = 10-12$ μs and $\tau_{rec,slow} = 20-25$ μs. The identity of the two recovery processes cannot be unambiguously defined without further measurements in which the grain diameter of the nanowires is varied, but it is likely that the faster of these two processes is electron−hole recombination at grain boundaries.[42] The photocurrent amplitude was strongly dependent on the optical power (Figure 4d) and this dependence is often described by a power law,[1,43] $i_{photo} = P^x$, where P is the optical power, c_1 is a proportionality constant, and c_2 is an empirical value that may be either larger than

DOI: 10.1021/nl100483v | *Nano Lett.* **2010,** *10,* 1481−1485

or smaller than unity. We measure a value for $c_2 = 0.93$, implying that the photocurrent is nearly proportional to the incident optical power (Figure 4e). This functionality, which is frequently seen for CdS,[44] is consistent with the presence of a low density of trap states arrayed in energy between the Fermi level (at midgap) and the conduction band edge.[44]

Presumably, *nc*-CdSe nanowires reduce response and recovery times to the microsecond range by reducing the lifetime, τ, of photoexcited carriers, a consequence of the rapid recombination of photogenerated electron−hole pairs at grain boundaries. Unfortunately, the depression of τ by this mechanism also limits the attainable photoconductive gain, G, defined as $G =$ photoelectrons/absorbed photons $= (I_{photo}/P_{optical})(h\nu/q) = \tau/t_r$ where t_r is the transit time for photoexcited carriers from contact to contact through the nanowire.[16,25,42] We estimate G values in the range from 0.032 to 0.050 depending on the optical power (Figure 4f), substantially lower than gain values seen for other nanowire systems or for CdSe films. In these nanowires, 20−30 photons must be absorbed by the array of *nc*-CdSe nanowires before a single electron is added to the current in the external circuit.

In summary, we have described an adaptation of the LPNE method for patterning ultralong *nc*-CdSe nanowires, with a mean grain diameter of 10 nm, onto glass. These nanowires have rectangular cross sections with adjustable widths (from 50 to 350 nm) and heights (20−80 nm). The photoconductivity of arrays of 350 nanowires, 60 nm × 200 nm in size, is characterized by photosensitivity factors of 10−100, response and recovery times of 20−40 μs, and photoconductive gain of 0.032−0.050. A remaining challenge is to understand and optimize the performance of these nanomaterials as a function of the mean grain diameter.

Acknowledgment. This work was supported by the National Science Foundation Grant DMR-0654055, the Petroleum Research Fund of the American Chemical Society 46815-AC 10, and the UCI School of Physical Sciences Center for Solar Energy.

REFERENCES AND NOTES

(1) Kind, H.; Yan, H.; Messer, B.; Law, M.; Yang, P. *Adv. Mater.* **2002**, *14*, 158–160.
(2) Law, M.; Kind, H.; Messer, B.; Kim, F.; Yang, P. *Angew. Chem., Int. Ed.* **2002**, *41*, 2405–2408.
(3) He, J. H.; Chang, P. H.; Chen, C. Y.; Tsai, K. T. *Nanotechnology* **2009**, *20*, 135701.
(4) Zhou, J.; Gu, Y.; Hu, Y.; Mai, W.; Yeh, P.-H.; Bao, G.; Sood, A. K.; Polla, D. L.; Wang, Z. L. *Appl. Phys. Lett.* **2009**, *94*, 191103. 3pp.
(5) Prades, J. D.; Jimenez-Diaz, R.; Hernandez-Ramirez, F.; Fernandez-Romero, L.; Andreu, T.; Cirera, A.; Romano-Rodriguez, A.; Cornet, A.; Morante, J. R.; Barth, S.; Mathur, S. *J. Phys. Chem. C* **2008**, *112*, 14639–14644.
(6) Ahn, S.-E.; Ji, H. J.; Kim, K.; Kim, G. T.; Bae, C. H.; Park, S. M.; Kim, Y.-K.; Ha, J. S. *Appl. Phys. Lett.* **2007**, *90*, 153106.
(7) Heo, Y.; Kang, B.; Tien, L.; Norton, D.; Ren, F.; Roche, J. L.; Pearton, S. *Appl. Phys. A: Mater. Sci. Process.* **2005**, *80*, 497–499.
(8) Park, D.; Yong, K. *J. Vac. Sci. Technol., B* **2008**, *26*, 1933–1936.
(9) Li, Y.; Dong, X.; Cheng, C.; Zhou, X.; Zhang, P.; Gao, J.; Zhang, H. *Physica B* **2009**, *404*, 4282–4285.
(10) Li, Y.; Valle, F. D.; Simonnet, M.; Yamada, I.; Delaunay, J.-J. *Nanotechnology* **2009**, *20*, No. 045501.
(11) Keem, K.; Kim, H.; Kim, G.-T.; Lee, J. S.; Min, B.; Cho, K.; Sung, M.-Y.; Kim, S. *Appl. Phys. Lett.* **2004**, *84*, 4376–4378.
(12) Lee, J.-S.; Sim, S.-K.; Min, B.; Cho, K.; Kim, S. W.; Kim, S. *J. Cryst. Growth* **2004**, *267*, 145–149.
(13) Liu, Z.; Zhang, D.; Han, S.; Li, C.; Tang, T.; Jin, W.; Liu, X.; Lei, B.; Zhou, C. *Adv. Mater.* **2003**, *15*, 1754–1757.
(14) Feng, P.; Zhang, J. Y.; Li, Q. H.; Wang, T. H. *Appl. Phys. Lett.* **2006**, *88*, 153107.
(15) Han, S.; Jin, W.; Zhang, D.; Tang, T.; Li, C.; Liu, X.; Liu, Z.; Lei, B.; Zhou, C. *Chem. Phys. Lett.* **2004**, *389*, 176–180.
(16) Jie, J. S.; Zhang, W. J.; Jiang, Y.; Meng, X. M.; Li, Y. Q.; Lee, S. T. *Nano Lett.* **2006**, *6*, 1887–1892.
(17) Liu, Y.; Zhou, X.; Hou, D.; Wu, H. *J. Mater. Sci.* **2006**, *41*, 6492–6496.
(18) Gao, T.; Li, Q. H.; Wang, T. H. *Appl. Phys. Lett.* **2005**, *86*, 173105.
(19) Chen, J.; Xue, K.; An, J.; Tsang, S.; Ke, N.; Xu, J.; Li, Q.; Wang, C. *Ultramicroscopy* **2005**, *105*, 275–280, Proceedings of the Sixth International Conference on Scanning Probe Microscopy, Sensors and Nanostructures.
(20) Li, Q.; Penner, R. M. *Nano Lett.* **2005**, *5*, 1720–1725.
(21) Fan, Z.; Ho, J. C.; Jacobson, Z. A.; Razavi, H.; Javey, A. *Proc. Natl. Acad. Sci. U.S.A.* **2008**, *105*, 11066–11070.
(22) Jiang, Y.; Zhang, W. J.; Jie, J. S.; Meng, X. M.; Fan, X.; Lee, S.-T. *Adv. Funct. Mater.* **2007**, *17*, 1795–1800.
(23) Pena, D. J.; Mbindyo, J. K. N.; Carado, A. J.; Mallouk, T. E.; Keating, C. D.; Razavi, B.; Mayer, T. S. *J. Phys. Chem. B* **2002**, *106*, 7458–7462.
(24) Calarco, R.; Marso, M.; Richter, T.; Aykanat, A. I.; Meijers, R.; v.d.Hart, A.; Stoica, T.; Luth, H. *Nano Lett.* **2005**, *5*, 981–984.
(25) Soci, C.; Zhang, A.; Xiang, B.; Dayeh, S. A.; Aplin, D. P. R.; Park, J.; Bao, X. Y.; Lo, Y. H.; Wang, D. *Nano Lett.* **2007**, *7*, 1003–1009.
(26) Singh, A.; Li, X.; Protasenko, V.; Galantai, G.; Kuno, M.; Xing, H. G.; Jena, D. *Nano Lett.* **2007**, *7*, 2999–3006.
(27) Zhou, R.; Chang, H.-C.; Protasenko, V.; Kuno, M.; Singh, A. K.; Jena, D.; Xing, H. G. *J. Appl. Phys.* **2007**, 101.
(28) Yu, Y.; Protasenko, V.; Jena, D.; Xing, H. G.; Kuno, M. *Nano Lett.* **2008**, *8*, 1352–1357.
(29) Capon, J.; Baets, J. D.; Rycke, I. D.; Smet, H. D.; Doutreloigne, J.; Calster, A. V.; Vanfleteren, J. *Sens. Actuators. A* **1993**, *37−38*, 546–551.
(30) Capon, J.; Baets, J. D.; Cubber, A. M. D.; Smet, H. D.; Calster, A. V.; Vanfleteren, J. *Phys. Status Solidi A* **1994**, *142*, 127–140.
(31) Menke, E. J.; Thompson, M. A.; Xiang, C.; Yang, L. C.; Penner, R. M. *Nat. Mater.* **2006**, *5*, 914–919.
(32) Xiang, C.; Kung, S. C.; Taggart, D. K.; Yang, F.; Thompson, M. A.; Guell, A. G.; Yang, Y.; Penner, R. M. *ACS Nano* **2008**, *2*, 1939–1949.
(33) Xiang, C.; Yang, Y.; Penner, R. M. *Chem. Commun.* **2009**, 859–873.
(34) Klein, J. D.; Herrick, R. D.; Palmer, D.; Sailor, M. J.; Bnunlik, C. J.; Martin, C. R. *Chem. Mater.* **1993**, *5*, 902–904.
(35) Schierhorn, M.; Boettcher, S. W.; Ivanovskaya, A.; Norvell, E.; Sherman, J. B.; Stucky, G. D.; Moskovits, M. *J. Phys. Chem. C* **2008**, *112*, 8516–8520.
(36) Kressin, A. M.; Doan, V. V.; Klein, J. D.; Sailor, M. J. *Chem. Mater.* **1991**, *3*, 1015–1020.
(37) Li, Q.; Brown, M. A.; Hemminger, J. C.; Penner, R. M. *Chem. Mater.* **2006**, *18*, 3432–3441.
(38) Menke, E. J.; Brown, M. A.; Li, Q.; Hemminger, J. C.; Penner, R. M. *Langmuir* **2006**, *22*, 10564–10574.
(39) Yang, Y.; Kung, S. C.; Taggart, D. K.; Xiang, C.; Yang, F.; Brown, M. A.; Guell, A. G.; Kruse, T. J.; Hemminger, J. C.; Penner, R. M. *Nano Lett.* **2008**, *8*, 2447–2449.
(40) Patterson, A. L. *Phys. Rev.* **1939**, *56*, 978–982.
(41) Devore, H. *Phys. Rev.* **1956**, *102*, 86–91.
(42) Sze, S. M.; Ng, K. K. *Physics of Semiconductor Devices*, 3rd ed.; Wiley & Sons: Hoboken, NJ, 2007.
(43) Joshi, N. V. *Photoconductivity: art, science, and technology*; Marcel Dekker: New York, 1990.
(44) Rose, A. *Concepts in Photoconductivity and Allied Problems*; Interscience: New York, 1963; Vol. 19.
(45) Sato, M.; Kawai, S.; Yamada, F. *Electrocomponent Sci. Technol.* **1981**, *8*, 199–206.
(46) Raturi, A.; Thangaraj, R.; Ram, P.; Tripathi, B.; Agnihotri, O. *Thin Solid Films* **1983**, *106*, 257–261.
(47) Garcia, V. M.; Nair, M. T. S.; Nair, P. K.; Zingaro, R. A. *Semicond. Sci. Technol.* **1996**, *11*, 427–432.
(48) Wang, X.; Wang, J.; Zhou, M.; Zhu, H.; Wang, H.; Cui, X.; Xiao, X.; Li, Q. *J. Phys. Chem. C* **2009**, *113*, 16951–16953.

DOI: 10.1021/nl100483v | *Nano Lett.* **2010,** *10,* 1481–1485